

This article was downloaded by:

On: 25 January 2011

Access details: Access Details: Free Access

Publisher Taylor & Francis

Informa Ltd Registered in England and Wales Registered Number: 1072954 Registered office: Mortimer House, 37-41 Mortimer Street, London W1T 3JH, UK



Separation Science and Technology

Publication details, including instructions for authors and subscription information:

<http://www.informaworld.com/smpp/title~content=t713708471>

Adsorption Behavior of Nano Sized Sol-Gel Derived $\text{TiO}_2\text{-SiO}_2$ Binary Oxide in Removing Pb^{2+} Metal Ions

A. Nilchi^a; S. Rasouli Garmarodi^a; S. Janitabar Darzi^b

^a Nuclear Science and Technology Research Institute, Tehran, Iran ^b Department of Chemistry, Faculty of Sciences, Tarbiat Modares University, Tehran, Iran

Online publication date: 22 March 2010

To cite this Article Nilchi, A. , Garmarodi, S. Rasouli and Darzi, S. Janitabar(2010) 'Adsorption Behavior of Nano Sized Sol-Gel Derived $\text{TiO}_2\text{-SiO}_2$ Binary Oxide in Removing Pb^{2+} Metal Ions', Separation Science and Technology, 45: 6, 801 – 808

To link to this Article: DOI: 10.1080/01496390903562332

URL: <http://dx.doi.org/10.1080/01496390903562332>

PLEASE SCROLL DOWN FOR ARTICLE

Full terms and conditions of use: <http://www.informaworld.com/terms-and-conditions-of-access.pdf>

This article may be used for research, teaching and private study purposes. Any substantial or systematic reproduction, re-distribution, re-selling, loan or sub-licensing, systematic supply or distribution in any form to anyone is expressly forbidden.

The publisher does not give any warranty express or implied or make any representation that the contents will be complete or accurate or up to date. The accuracy of any instructions, formulae and drug doses should be independently verified with primary sources. The publisher shall not be liable for any loss, actions, claims, proceedings, demand or costs or damages whatsoever or howsoever caused arising directly or indirectly in connection with or arising out of the use of this material.

Adsorption Behavior of Nano Sized Sol-Gel Derived $\text{TiO}_2\text{-SiO}_2$ Binary Oxide in Removing Pb^{2+} Metal Ions

A. Nilchi,¹ S. Rasouli Garmarodi,¹ and S. Janatabar Darzi²

¹*Nuclear Science and Technology Research Institute, Tehran, Iran*

²*Department of Chemistry, Faculty of Sciences, Tarbiat Modares University, Tehran, Iran*

Nanostructure Titania-Silica ($\text{TiO}_2\text{/SiO}_2$) binary mixed oxide was synthesized using titanium tetra chloride and tetraethylorthosilicate as starting materials. The resulting powder was characterized by thermogravimetry-differential scanning calorimetry (TG-DSC), X-ray powder diffraction (XRD), X-ray fluorescence spectroscopy (XRF), infrared spectroscopy (IR), transmission electron microscope (TEM), and nitrogen gas adsorption studies. The XRD and BET surface area showed that the Titania-Silica binary oxide was crystallized in the anatase and brookite phases and had a BET surface area of $405.3 \text{ m}^2/\text{g}$. Distribution coefficient of Pb^{2+} ions in solid and liquid phases were investigated by means of batch experiments. Several parameters such as the contact time and the pH of the solution, which could affect the magnitude of adsorption, were examined. Sorption data have been interpreted in terms of the Freundlich and Langmuir equations. The results of free energy (ΔG°), enthalpy (ΔH°), and entropy (ΔS°) showed that the sorption of Pb^{2+} on $\text{TiO}_2\text{-SiO}_2$ is an endothermic and a spontaneous process.

Keywords adsorption; binary mixed oxide; heavy metal ions; lead; $\text{TiO}_2\text{-SiO}_2$

INTRODUCTION

The presence of heavy metals in the environment is a serious global, social, and environmental problem. Many industrial facilities, such as metal plating, mining operations, fertilizer industry, tanneries, and textile industries, discharge heavy metals via their waste effluents. The toxic metal ions are a serious health hazard and every possible care should be taken to keep them isolated from getting mixed into air, water, and soil.

High levels of lead damages brain and kidney, mercury vapors leads to permanent brain damage at high concentration levels, higher concentration of copper in water can cause eye irritation, headache, dizziness, and diarrhea and inhaling too much chromium cause fragile bones and probably a human carcinogen.

Received 25 February 2009; accepted 9 December 2009.

Address correspondence to A. Nilchi, Nuclear Science and Technology Research Institute, P.O. Box 11365/8486, Tehran, Islamic Republic of Iran. Tel.: (+98) 21 88221128; Fax: (+98) 21 82062539. E-mail: anilchi@aeoi.org.ir

As an effort to reduce the heavy metal levels in waste water, drinking water and water used for agriculture to the maximum permissible concentration, therefore, several methods such as ion exchange/adsorption, precipitation, and membrane separation have been adopted (1–7). Among various techniques, the ion exchange process is used exclusively in water treatment and many studies have been carried out to find inexpensive and chemico-physically feasible adsorbers. Therefore, for an ion exchanger to be practical in the removal of heavy metals from industrial wastewater containing other competing ions such as calcium and magnesium, it is essential that the chosen sorbent be sufficiently selective toward heavy metals against calcium and magnesium.

Extensive studies on the adsorption and ion-exchange properties of hydrous oxides have been carried out from the point of view of analytical separation, adsorbents for the recovery of trace metals present in natural waters and matrices for radioactive nuclear wastes (8). Ion-exchange and adsorption properties of hydrous oxides arise from the pH dependent protonation and deprotonation reactions of surface hydroxyl groups, when in contact with solution (9).

Titania-Silica mixed oxide is an interesting material for the adsorption of certain metal ions since the cation exchange property of silica and both cation and anion exchange properties of titania are well known. The co-precipitation of titanium oxide and silica oxide, seriously affect the surface properties (specific surface area, porosity, acidic sites, etc.) of each component, which provides a supplementary influence on the adsorption (10,11).

In the present study, the preparation of nanostructure $\text{TiO}_2\text{-SiO}_2$ mixed oxide and the application of this highly efficient adsorbent in the removal of Pb^{2+} ions is discussed.

EXPERIMENTAL

Reagents

Titanium (IV) chloride (98% Fluka), tetraethylorthosilicate (98% Merck), and ammonium hydroxide (25% Fluka) were used as the starting materials without further purification. Merck analytical grade nitrate salt of Pb^{2+} was used to prepare the stock solution.

Adsorbent Preparation

For TiO_2 preparation, TiCl_4 was added dropwise to deionized water under vigorous stirring in an ice water bath. The hydrolysis reaction was highly exothermic and HCl was released. The produced dispersion was treated with NH_4OH and pH was adjusted to 7. The resulting solid was collected by filtration and washed with deionized water in order to remove the chlorine ions.

For $\text{TiO}_2\text{-SiO}_2$ preparation, the precipitate was dispersed in 200 mL of 0.3 mol/L HNO_3 . The mixture was refluxed under vigorous stirring at 70°C for 16 h as Titania sol was prepared. 25 mL of tetraethylorthosilicate was added dropwise to the above sol and stirred at 70°C. The resulting powder was filtered and washed with deionized water and then dried at room temperature. The prepared mixed oxide was calcined in air, at 400°C for 1 h, with a heating rate of 10°C/min.

Characterization

In order to determine the structure of the adsorber, X-ray powder diffractometry was carried out using an 1800 PW Philips diffractometer with $\text{CuK}\alpha$ beam. The finely powdered sample of the adsorber was packed in a flat aluminium sample holder, where the X-ray source was a rotating anode operating at 40 kV and 30 mA with a copper target. Data were collected between 20 and 80 degrees in 2Θ ; the average crystallite sizes of synthesized sample was determined by employing the Scherrer equation,

$$D = K\lambda/(\beta \cos \Theta) \quad (1)$$

where D is the average crystallite size (nm), λ is the applied X-ray wavelength ($\lambda = 1.5406 \text{ \AA}$), Θ is the diffraction angle, and β is a full width at half the maximum of diffraction line observed in radians; the infrared spectra were recorded using a Brucker-Vector22 spectrometer; the amount of each component of the prepared sample was determined by X-ray fluorescence spectroscopy (XRF) using an Oxford ED 2000; the transmission electron micrograph was taken using a TEM, Philips EM208S; Brunauer-Emmett-Teller (BET) specific surface area and Barret-Joyner-Halenda (BJH) pore size distribution of the sample was determined through nitrogen adsorption isotherms using Quantachrome NOVA 2200e system and thermogravimetry-differential scanning calorimetry (TG-DSC) was carried out using STA 150 Rhenometric Scientific unit, measurements were taken with a heating rate of 10°C/min from 25 to 800°C in argon atmosphere.

Zeta Potential Measurements

The Zeta potential measurements of nanostructure $\text{TiO}_2\text{-SiO}_2$ were carried out by using aqueous suspensions which were prepared by adding 0.05 g of the nano-sample to 1 L of 0.01 mol/L NaCl . The pH was adjusted to the

desired value by adding HNO_3 or NaOH . These suspensions were shaken for 60 min. The zeta potentials was measured using Zetameter (Zetameter Inc., USA) and also the final pH of the suspensions was recorded with a Schott CG841 pH-meter.

Batch Experiments

The amount of metal ion adsorbed was expressed in terms of the distribution coefficient (K_d). The distribution coefficient is defined as the concentration sorbed per gram of the sorbent divided by its concentration per mL at equilibrium. The higher K_d implies a higher selectivity or adsorption. Pb^{2+} ions remaining in the solution were measured by inductively coupled plasma atomic emission (ICP-AES) spectrometer model 5500 Perkin-Elmer.

The Effect of Contact Time on K_d

The adsorption of Pb^{2+} on the mixed oxide was studied as a function of contact time at pH 7 and 25°C. 25 mL of 10^{-4} mol/L solution of cation was shaken with 0.10 g of the synthesized sample for different time intervals, ranging from 10 to 120 min. The supernatant solutions were filtered and concentration of Pb^{2+} cation was determined by ICP-AES.

The Effect of pH

In order to investigate the effect of pH of solution on the distribution coefficient of Pb^{2+} ions, 10^{-4} mol/L solutions of cation at different pH values were prepared. 25 mL of these solutions were added to 0.10 g of adsorbent at 25°C. After the equilibrium was reached, the supernatant solutions were filtered and the concentration of Pb^{2+} was determined.

Effect of Thermal Treatment Temperature of Mixed Oxide

The mixed oxide were calcined in air, at 400, 600, 800, 950, and 1100°C, for 1 h. Twenty-five mL of 10^{-4} mol/L lead nitrate solution was treated with 0.10 g of the mixed oxide for each treatment temperature, at pH 6.0, in a thermostatically controlled shaker, at 25°C, for a specific period of contact time. The final concentration of Pb^{2+} was determined by ICP-AES and its distribution coefficient was calculated.

Isotherm Studies

The investigation of adsorption isotherm was conducted by batch process. Pb^{2+} solutions at different concentrations were prepared and the pH values of these solutions were adjusted to 6.0. 0.10 g of the mixed oxide was added to each sample. The samples were treated in a thermostatically controlled shaker at 25, 35, and 52°C (298, 308, and 325 K), for 60 min. The supernatants solutions were filtered and the concentration of Pb^{2+} ions was determined. The quantity of the adsorbed cation on the $\text{TiO}_2\text{-SiO}_2$ mixed

oxide was calculated using the formula given below:

$$q_e = \frac{(C_0 - C_e)V}{M} \quad (2)$$

where C_0 and C_e are the initial and equilibrium concentrations of metal ion in the solution, V is the volume of solution (mL), and M is the weight of the ion exchanger in contact with solution (g).

RESULTS AND DISCUSSION

Characterization of $\text{TiO}_2\text{-SiO}_2$

IR spectra of $\text{TiO}_2\text{-SiO}_2$ sample calcined at 400°C is shown in Fig. 1. The band at around 1100 cm^{-1} is the asymmetrical vibration of the Si-O-Si bond in the tetrahedral SiO_4 unit of the SiO_2 matrix. The symmetrical Si-O-Si stretching vibration appeared at 795 cm^{-1} , along with a peak at 954 cm^{-1} ; this band has been ascribed to the vibration involving a SiO_4 tetrahedron bonded to a titanium atom through Si-O-Ti bonds. The presence of this band confirms the presence of the Si-O-Ti linkages in the synthesized product. The $\text{TiO}_2\text{-SiO}_2$ sample exhibit a band at around 490 cm^{-1} which is representative of the TiO_2 matrixes. The broad band in the region of $3200\text{--}3650\text{ cm}^{-1}$ is due to the stretching vibration of hydroxyl groups and interlayer water molecules; the peak at 1620 cm^{-1} can be assigned to the deformation vibration of the free water molecules.

Figure 2 depicts the XRD pattern of the sample calcined at 400°C . It reveals that as-synthesized $\text{TiO}_2\text{-SiO}_2$ has crystalline anatase phase beside brookite in amorphous silica matrix. The existence of brookite in XRD pattern is clearly evidenced from the presence of the peak at $2\Theta = 30.81^\circ$. For the interpretation of the diffractograms, it is necessary to take into account that the main diffraction peak of anatase at $2\Theta = 25.28^\circ$ overlaps with the peaks of brookite at $2\Theta = 25.34^\circ$ and 25.69° , respectively (12). The size of the anatase crystallites in the prepared sample measured according to the Scherrer equation is 5.09 nm.

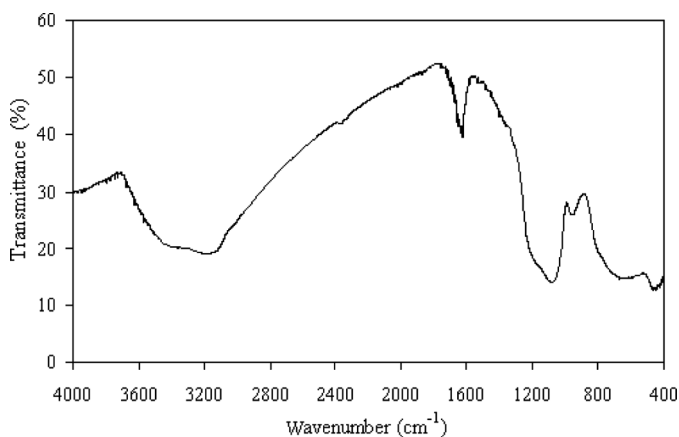


FIG. 1. IR spectra of Titania-Silica binary mixed oxide.

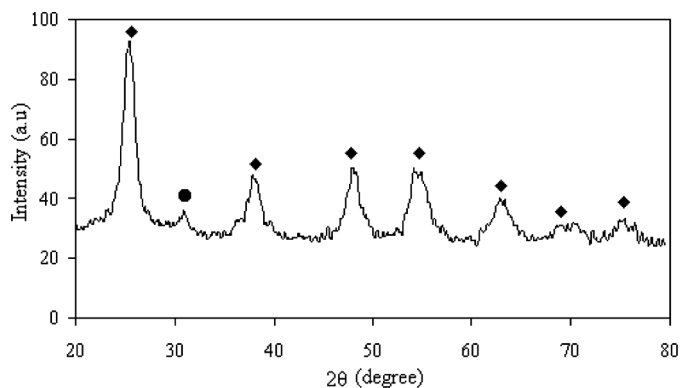


FIG. 2. XRD pattern of $\text{TiO}_2\text{-SiO}_2$. (■) peaks due to anatase, (●) peak due to brookite.

The XRF analysis shows that the Titania-Silica mixed oxide calcined at 400°C consists of 50% TiO_2 and 46% SiO_2 .

N_2 adsorption-desorption isotherm and pore size distribution analysis of synthesized oxide calcined at 400°C are illustrated in Fig. 3. The isotherm of $\text{TiO}_2\text{-SiO}_2$ is type IV, indicating the presence of mesopore. The hysteresis loop is a H_2 type with a triangular shape and a steep desorption branch. Such behavior is observed for many porous inorganic oxides and has been attributed to the pore connectivity effects (13). Indeed, the H_2 hysteresis loops have been observed for materials with relatively uniform channel-like pores, when the desorption branch happened to be in the proximity of a lower pressure limit of adsorption-desorption hysteresis (14). The shape of the hysteresis loop for this binary oxide clearly indicates some pore blocking, as the almost horizontal plateau of adsorption ends. Therefore, it can be concluded that the porosity of the sample is characterized by some cavities which are connected with each other and with the external surface via narrow pores,

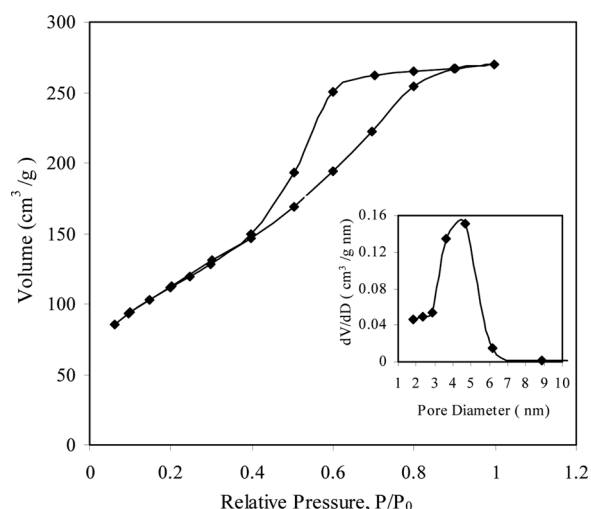


FIG. 3. Nitrogen adsorption-desorption isotherm and the BJH pore diameter curve of $\text{TiO}_2\text{-SiO}_2$.

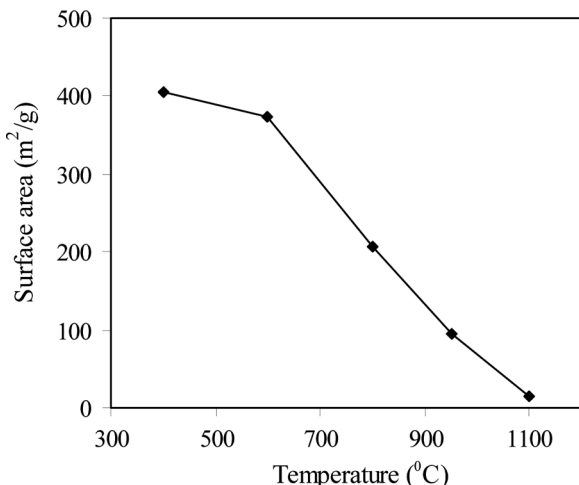


FIG. 4. Surface area of $\text{TiO}_2\text{-SiO}_2$ mixed oxide calcined at different temperatures.

the so-called ink-bottle type of porosity. The cavities are being created by the partial decomposition of the organosiliceous component of the material. The results revealed that the prepared material had a BET surface area of up to $405.3 \text{ m}^2/\text{g}$; and according to BJH plot the pore diameter of mixed oxide was obtained around 4.65 nm.

The BET surface area of the $\text{TiO}_2\text{-SiO}_2$ samples calcined at different temperatures is given in Fig. 4. The surface area decreases from 405.3 to $14.78 \text{ m}^2/\text{g}$ with increasing calcinations temperature up to 1100°C . The decrease of the surface area upon calcination is due to the crystallization of the walls separating mesopores.

It can be seen from the TEM micrograph of the synthesized material (calcined at 400°C) that the granular TiO_2 nanocrystallites (deep dark spots) are dispersed in the amorphous SiO_2 matrix (Fig. 5). The image also shows the particle size of the adsorber was less than 10 nm on average.

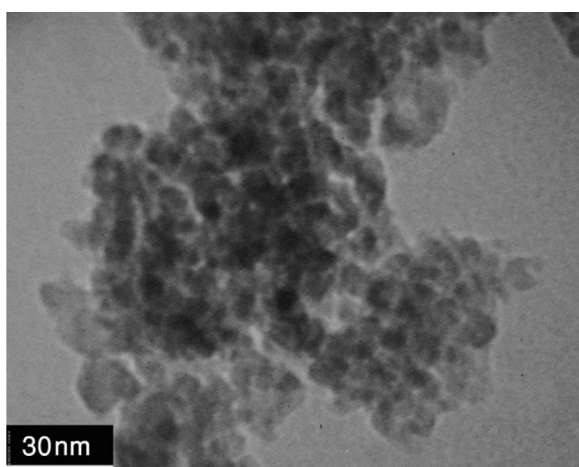
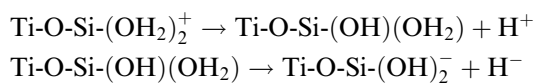


FIG. 5. TEM micrograph of synthesized $\text{TiO}_2\text{-SiO}_2$.

Differential scanning calorimetry and thermogravimetric curves of as-synthesized $\text{TiO}_2\text{-SiO}_2$ calcined at 400°C are shown in Fig. 6. The decrease in weight, up to 150°C is attributed to the desorption of the physisorbed water and organic residue (confirmed by an endothermic peak on the DSC curve at about 100°C). A diffuse exotherm at around 400°C is the result of the small portion of anatase crystallizing to brookite. Above 400°C , the change in weight is very small.

Zeta Potential and Isoelectric Point of $\text{TiO}_2\text{-SiO}_2$

The pH value strongly influences the surface charge properties of metal-oxide particles in the aqueous dispersion. The surface sites in terms of the neutral and unoccupied surface sites of TiO_2 can be represented as $\text{Ti}(\text{OH})(\text{OH}_2)$, having both a surface hydroxyl and a chemisorbed water (15). Therefore, the acid–base properties of the $\text{TiO}_2\text{-SiO}_2$ /water interface can be described by

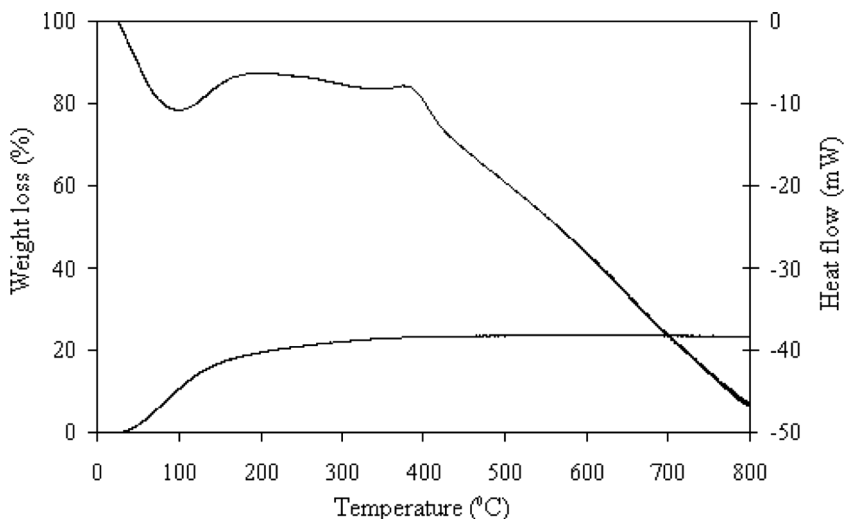
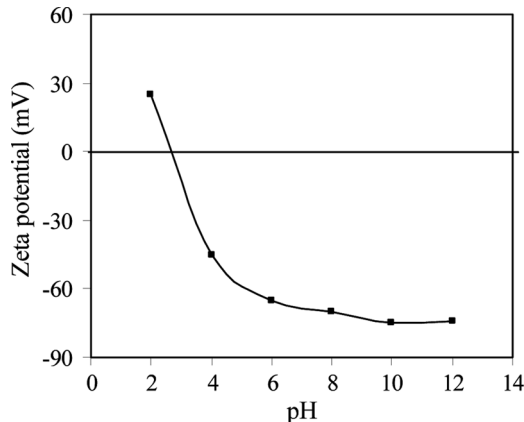
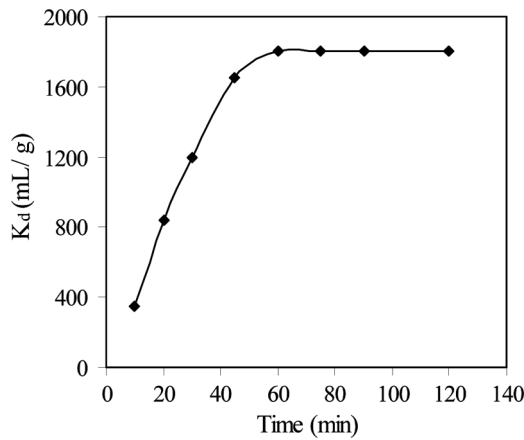


where $\text{Ti-O-Si-(OH}_2\text{)}_2^+$, $\text{Ti-O-Si-(OH)(OH}_2\text{)}$, and Ti-O-Si-(OH)_2^- are protonated, neutral, and deprotonated titanium dioxide surface sites, respectively. The above-mentioned species, which function in the pH, play an important role in the sorption on the surface of the mixed oxide. Therefore, the effect of pH on the surface species and consequently on the surface charge can be represented by measuring zeta potential of $\text{TiO}_2\text{-SiO}_2$. Figure 7 indicates that the PZC of $\text{TiO}_2\text{-SiO}_2$, 2.8, is closer to the values of silica's PZC reported in the literature which ranges from 1.8 to about 3.5 than that of titania which is 6.5 (16). With the increase of pH, the zeta potential changes from positively charged at pH below 2.8 to negatively charged above 2.8 as shown in Fig. 7, which indicates the presence of the protonated species below pH 2.8, and deprotonated above pH 2.8.

Adsorption Properties

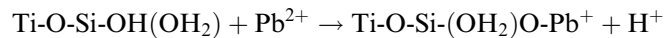
The distribution coefficient of Pb^{2+} as a function of time (Fig. 8) were used to determine an optimum contact time for the adsorption of lead ions onto $\text{TiO}_2\text{-SiO}_2$. As it can be seen, there is a rapid uptake within 45 min and the adsorption equilibrium is attained within 60 min.

pH is an important parameter influencing heavy metal adsorption from aqueous solutions. It affects both the surface charge of the adsorbent and the degree of ionization of the heavy metal in solution. Figure 9 represents the effect of initial pH of the solution on K_d of Pb^{2+} ions. The distribution coefficient values were found to be higher with increased pH values. The optimum pH value at which the maximum adsorption could be achieved was 6.0. For all subsequent experiments, this optimum pH value was used.

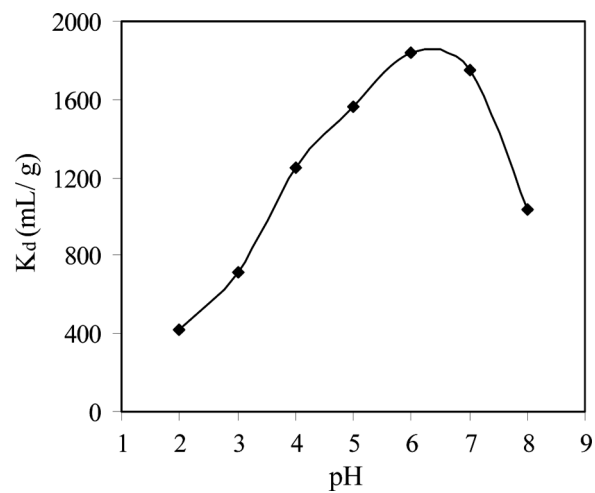
FIG. 6. TG-DSC curves of $\text{TiO}_2\text{-SiO}_2$.FIG. 7. Zeta potential of $\text{TiO}_2\text{-SiO}_2$ at different pH.FIG. 8. Effect of contact time on K_d of Pb^{2+} metal ions.

At pH values higher than 8.0 insoluble lead hydroxide starts precipitating from the solution making true sorption studies impossible.

In order to understand the adsorption mechanism, the variation of the solution pH during the lead adsorption was measured as in Fig. 10. A decrease in pH was observed during the sorption processes, which suggests there was a simultaneous release of H^+ into the solution. It is proposed that the hydroxyl groups of silica, which need alkaline media to be formed, are involved in the formation of surface complexes with metal ions:



The binding of Pb^{2+} ions by surface functional groups begins at pH 2 and rises within the next pH units.

FIG. 9. Effect of pH of solution on K_d value of Pb^{2+} ions.

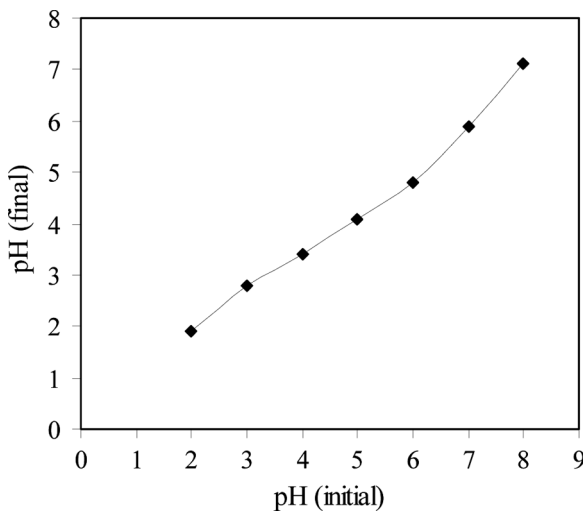


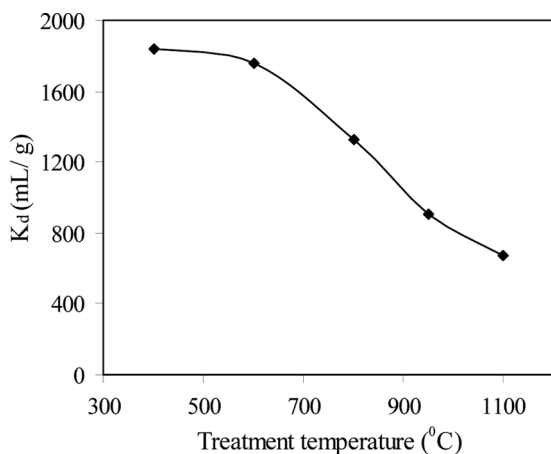
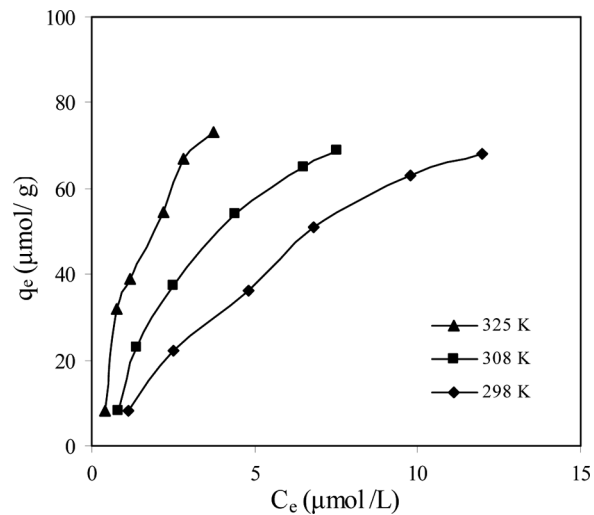
FIG. 10. Variation of pH of aqueous solutions with lead adsorption.

This suggests that a reaction of Pb^{2+} ions with the $\text{TiO}_2\text{-SiO}_2$ surface involves bond formation via surface oxygen atoms and proton release.

The relation of the distribution coefficient of Pb^{2+} on the adsorbent with thermal treatment of oxide spheres is given in Fig. 11. As it can clearly be seen, the K_d values decrease with the increasing calcination temperatures. These results are in good conformity to the BET surface area of the $\text{TiO}_2\text{-SiO}_2$ samples.

Adsorption Isotherms

The adsorption isotherms are mathematical models that describe the distribution of the adsorbate species among the liquid and the adsorbent, based on a set of assumptions that are mainly related to the heterogeneity/homogeneity of adsorbents, the type of coverage, and the possibility of interaction between the adsorbate species. The Langmuir

FIG. 11. Effect of thermal treatment of $\text{TiO}_2\text{-SiO}_2$ on K_d values.FIG. 12. Adsorption isotherm of Pb^{2+} on $\text{TiO}_2\text{-SiO}_2$.

model assumes that there is no interaction between the adsorbate molecules, and the adsorption is localized in a monolayer. The Freundlich isotherm model is an empirical relationship describing the adsorption of solutes from a liquid to a solid surface, and assumes that different sites with several adsorption energies are involved.

The adsorption isotherm of Pb^{2+} ions on $\text{TiO}_2\text{-SiO}_2$ is represented in Fig. 12. The experimental data of lead adsorption were analyzed with the Freundlich and Langmuir models. The equations of the Freundlich and Langmuir adsorption models are expressed, respectively (17,18).

$$\log q_e = \log K_F + \frac{1}{n} \log C_e \quad (3)$$

$$\frac{C_e}{q_e} = \frac{1}{Q^\circ b} + \frac{C_e}{Q^\circ} \quad (4)$$

where C_e is the equilibrium solution phase concentration ($\mu\text{mol/L}$), q_e is the equilibrium solid phase concentration ($\mu\text{mol/g}$), Q° is the maximum adsorption ($\mu\text{mol/g}$), and b is the constant related to the free energy of adsorption. Finally, K_F is the constant indicative of the relative ion exchange capacity of the adsorbent ($\text{mol}^{1-1/n} \text{L}^{1/n}/\text{g}$) and $1/n$ is the constant indicative of the intensity of the ion exchange/adsorption.

The parameters calculated from the Freundlich and Langmuir models are summarized in Table 1. The higher correlation coefficients indicate that the Langmuir model fits the adsorption data better than the Freundlich model. Moreover, $\text{TiO}_2\text{-SiO}_2$ had a limited adsorption capacity, thus the adsorption could be better described by the Langmuir model rather than by the Freundlich model, as an exponentially increasing adsorption was assumed in the Freundlich model.

TABLE 1
Parameters of the Langmuir and Freundlich models at various temperatures

T(K)	Langmuir constants			Freundlich constants		
	Q° (μmol/g)	b (L/μmol)	R ²	K _F (mol ^{1-1/n} L ^{1/n} /g)	1/n	R ²
298	97.46	0.05	0.99	1.18	0.87	0.98
308	169.77	0.10	0.99	2.46	0.90	0.98
325	203.25	0.78	0.96	0.13	0.59	0.96

Adsorption Thermodynamic

The thermodynamic parameters, the values of standard free energy (ΔG°), standard enthalpy (ΔH°), and standard entropy (ΔS°) of the sorption are useful in defining whether the sorption reaction is endothermic or exothermic, and the spontaneity of the adsorption process. The parameters can be calculated using the following equations (19):

$$\Delta G^\circ = -RT \ln K_1 \quad (5)$$

$$\ln \frac{K_1}{K_2} = -\frac{\Delta H^\circ}{RT} + \left(\frac{1}{T_1} - \frac{1}{T_2} \right) \quad (6)$$

$$\Delta S^\circ = \frac{\Delta H^\circ - \Delta G^\circ}{T} \quad (7)$$

where R (8.3145 J/mol K) is the ideal gas constant, and T(K) is the temperature. K is the apparent equilibrium constant corresponding to the temperature which may be calculated from the product of the Langmuir equation parameters Q° and b . So, the values of the constants K_1 , K_2 , and K_3 corresponding to the temperatures of 298, 308, and 325 K, respectively, are given in Table 2. Also, relevant data calculated from the above equations are tabulated in Table 2.

The adsorption of Pb^{2+} increases with the increase of temperature and the value of ΔH° is positive. The positive enthalpy value confirms that the adsorption process is endothermic for Pb^{2+} , which is an indication of the existence of a strong interaction between the adsorbent and lead cation. For Pb^{2+} ions to travel through the solution and reach the sorption sites, it is necessary for them first to

be stripped out (at least partially) of their hydration shell, this process requires energy input.

The Gibbs free energy change (ΔG°) was negative as expected for a spontaneous process under the conditions applied. The decrease in ΔG° with the increase of temperature indicated more efficient adsorption at higher temperature. At high temperature, the ions are readily dehydrated, and therefore their adsorption becomes more favorable.

The positive values of the entropy change (ΔS°) reflected the affinity of TiO_2 - SiO_2 toward Pb^{2+} ions in aqueous solutions and may suggest some structure changes in the adsorbents.

CONCLUSION

The overall results indicate the possibility of using the synthesized TiO_2 - SiO_2 mixed oxide for efficient removal of Pb^{2+} from aqueous solutions. As a result of the experimental conditions; it was shown that Pb^{2+} adsorption onto the prepared material is an endothermic and a spontaneous process. The fact that the Langmuir isotherm fits the experimental data better than the Freundlich model indicates the almost complete monolayer coverage of the adsorbent particles. The extent of sorption mainly depends on the surface charge as well as the species present in the solution.

REFERENCES

1. Oehmen, A.; Viegas, R.; Velizarov, S.; Reis, M.A.M.; Crespo, J.G. (2006) Removal of heavy metals from drinking water supplies through the ion exchange membrane bioreactor. *Desalination*, 199: 405–407.
2. Khan, A.A.; Inamuddin, A.A. (2006) Applications of Hg(II) sensitive polyaniline Sn(IV) phosphate composite cation-exchange material in determination of Hg^{2+} from aqueous solutions and in making ion-selective membrane electrode. *Sensors Actuat. B*, 120: 10–18.
3. Fatin-Rouge, N.; Dupont, A.; Vidonne, A.; Dejeu, J.; Fievet, P.; Foissy, A. (2006) Removal of some divalent cations from water by membrane-filtration assisted with alginate. *Water Res.*, 40: 1303–1309.
4. Zhang, F.S.; Nriagu, J.O.; Itoh, H. (2004) Photocatalytic removal and recovery of mercury from water using TiO_2 -modified sewage sludge carbon. *J. Photochem. Photobiol. A Chem.*, 167: 223–228.
5. Khalil, L.B.; Rophael, M.W.; Mourad, W.E. (2002) The removal of the toxic Hg(II) salts from water by photocatalysis. *Appl. Catal. B Environ.*, 36: 125–130.

TABLE 2
Thermodynamic parameters for Pb^{2+} adsorption onto TiO_2 - SiO_2

T(K)	K (L/g)	ΔG° (kJ/mol)	ΔH° (kJ/mol)	ΔS° (kJ/mol K)
298	$K_1 = 9.37$	-5.54		
308	$K_2 = 17.56$	-7.46	63.05	0.23
325	$K_3 = 75.64$	-11.62		

6. Matlock, M.M.; Howerton, B.S.; Atwood, D.A. (2002) Chemical precipitation of heavy metals from acid mine drainage. *Water Res.*, 36: 4757–4764.
7. Namasivayam, C.; Periasamy, K. (1993) Bicarbonate-treated peanut hull carbon for mercury (II) removal from aqueous solution. *Water Res.*, 27: 1663–1668.
8. Ruvarac, A. (1982) *Inorganic Ion Exchange Materials*. In: Clearfield, A. ed.; CRC Press, Inc.: Boca Raton, FL, 141–145.
9. Parks, G.A. (1965) The isoelectric points of solid oxides, solid hydroxides and aqueous hydroxo complex systems. *Chem. Rev.*, 65: 177–198.
10. Iler, R.K. (1978) *The Chemistry of Silica*; John Wiley & Sons: New York, 576–581.
11. Venkataramani, B. (1991) Ion exchange and sorption properties of hydroxides. In: *New Developments in Ion Exchange, Proceeding of International Conference on Ion Exchange, ICIE'91*, Abe, M.; Kataoka, T.; Suzuki, T., eds.; Tokyo, Japan, Elsevier, Amsterdam, 169–175.
12. Paola, A.; Cufalo, G.; Addamo, M.; Bellardita, M.; Campostrini, R.; Ischia, M.; Ceccato, R.; Palmisano, L. (2008) Photocatalytic activity of nanocrystalline TiO_2 (brookite, rutile and brookite-based) powders prepared by thermohydrolysis of $TiCl_4$ in aqueous chloride solutions. *J. Colloid Interface Sci. A: Physicochem. Eng. Aspects*, 317: 366–376.
13. Liu, H.; Zhang, L.; Seaton, N.A. (1993) Analysis of sorption hysteresis in mesoporous solids using a pore network model. *J. Colloid Interface Sci.*, 156: 285–293.
14. Krusk, M.; Jaroniec, M.; Sayari, A. (1997) Application of large pore MCM-41 molecular sieves to improve pore size analysis using nitrogen adsorption measurements. *Langmuir*, 13: 6267–6273.
15. Stone, T.A.; Torrents, A.; Smolen, J.; Vasudevan, D. (1993) Adsorption of organic compounds possessing ligand donor groups at the oxide/water interfaces. *Environ. Sci. Technol.*, 27: 895.
16. Bresson, C.; Menu, J.M.; Dartiguenave, M.; Dartiguenave, Y. (2000) Triethylsilyl-substituted aminoethanethiol ligands for zinc and cadmium complexes and aminoethanethiol-modified silica gel. Evaluation of corresponding supported molecular trap for metallic pollutant uptake (Cd^{2+} , Hg^{2+} and Pb^{2+}). *J. Environ. Monit.*, 2: 240–247.
17. Langmuir, I. (1916) The constitution and fundamental properties of solids and liquids. *J. Am. Chem. Soc.*, 38: 2221–2295.
18. Freundlich, H. (1906) Über die adsorption in Lösungen. *Z. Phys. Chem. A*, 57: 385–470.
19. Chen, C.; Li, X.; Zhao, D.; Tan, X.; Wang, X. (2007) Adsorption kinetic, thermodynamic and desorption studies of Th (IV) on oxidized multi-wall carbon nanotubes. *J. Colloid Interface Sci. A: Physicochem. Eng. Aspects*, 302: 449–454.